https://doi.org/10.36375/prepare_u.iei.a147

Tesseract Based Data Visualization Technique for Monitoring and management of COVID-19 Patients

Dr. Sayantan Nath, Dr. C. Mala

Department of Computer Science and Engineering
National Institute of Technology, Trichy
Tuvakudi, TN – 620015

{sayantan@nitt.edu, cmala@nitt.edu}

Abstract - A continuous process of monitoring of the clinical condition of COVID patients is proposed in this paper. The coined technique is fundamentally designed on the multi-dimensional data framework architecture. The measuring method of the continuous monitoring process for a greater number of patients with multiple sensors and medical devices in ICUs in a large hospital is very much difficult to manage and control. The regular health-care monitoring systems are mainly designed on the critical parameters of the patients. These constraints are also taken into account to design the key blocks for this framed Tesseract model with other parameters also e.g. number of wards etc. This model would not only help the doctors to check and analyze the medical data of the patients in a multi-dimensional format but also will help the hospital authority to manage and scrutiny the patient's database efficiently. This technique would be beneficial for both stakeholders of the medical field.

Keywords - Time-quantum, Data Tesseract, Continuous monitoring, multi-dimensional visualization, COVID patients

INTRODUCTION

Continuous health-care checking is being considered as one of the most critical monitoring factors in medical scenarios especially in developing countries where the population is huge. So, it is very essential to streamline the multi-vitiate medical data [1] with an increasing rate of COVID contamination. To rationalize this multi-constrains data-oriented process, this Tesseract model [2] has been proposed. The technical parameters related to medical data like physiological sensors attached to the body [3] of the patients are performing continuously. And in a larger hospital, multiple patients affected with COVID in the number of wards make the data handling scenario [4] more complex especially for the medical staff who is continuously trying their best to save a life. The basic difference from the traditional monitoring technique compared to the proposed model is that the old techniques only based upon the approaches of various data-science processes [5] like heat-map, 2D scatter plot, etc. which may be good in their calculative means.

However, the proposed architecture manages the best structural integrity between the medical parameters and statistical data [6] through the multi-dimensionality. The hospital authority is usually looking further to point-down any specific statistics related to the COVID patients to boost up their medical information database [7] and public information. And the doctors are looking for a smellier pattern in the patients so that treatment would be easy. In this multi-demanding, multi-crucial scenario, [8] an ideal stage for integrated medical data is very essential to be developed with all parameters that could be measured. The hospital authority and medical staff could handle the framed data [9] thoroughly and cultivates further knowledge as their requirements.

In the techniques, doctors can either examine the COVID patient or they could perform data analysis and follow higher authority [10] simultaneously. This proposed system helps to record the data interfacing [11] with each level of COVID patients with its serial number, ward, and physiological parameters.

In this study, it is has been observed that time scheduling for COVID patients monitoring based on the continuity of work in a hospital is not explored on a large scale [12]. The proposed system will also help the doctors to judge the contamination of the COVID patients in the ward which is often miscalculated by the authority [13].

In this process, the clinical parameters are highlighted by the critical factor [14] of engagement of COVID patients at the isolation center. The further contraction of data was

https://doi.org/10.36375/prepare_u.iei.a147

decreasing concerning the health quality of the COVID patients and forcing the doctors to recruit and retain more medical needs. Hospital's authority loses control of the data affectability [15] to gain the potential significance of the infectious rate over each level of patients [16].

In this technique, the overall percentage matches is an old medical modeling process [17], in 2008, an updated COVID patient monitoring system was introduced especially for the parameters-based data [18] related measurement technique. Those particular patterns in data had made a substantial impact on the relationship between doctors and medical staff. To help COVID patients for further restrains in the hospitals, monitoring [19] has begun to learn important information about each COVID carries. The hospital authority could calibrate those data and parameters with the old model [20].

In this method, the rechecking of the assessment factors of a COVID patient who becomes a top considerable medical emergency was analyzed for decision-making practices [21] by the doctors. If results were found align closely to the ideal condition, the validity of that COVID patient as recovering is good. However, if the results deviate significantly from the ideal condition, there might be a reason to re-calibrate [22] the importance of certain parameters of the COVID patients again.

This study is carried out to identify the dimensional aspects responsible for the successful design and implementation of an intelligent monitoring system [23] for COVID patients. Its system will be employed for all stages of monitoring with an equal preference for all number of COVID patients. On one hand, it accurately monitors the physical data of each COVID patient as well as on the other hand the data would be integrated with mathematical bonding [24] directly.

Designing of the Proposed Technique

In this proposed monitoring technique of COVID patients, new terminology is introduced as “time-quantum” which means the unit of monitoring duration. This time quantum factor could be divided or integrated according to the requirement of the medical advice. Such as, if the monitoring duration is 8 hours and the value of time-quantum, denoted as τ, is set as 30 sec, the total rate of data acquisition would be taken in total 8 hr. of monitoring would be, P = 8*60*60/30=960. So, in 8 hours of monitoring, a total of 960 cycles of data would be obtained. In this duration, if data would not be taken in a certain interval, then that blank in the dataset would also be recognized as a gap. In these 8 hours of duration, if data would not be acquired for 120 sec., the total number of cycles would be 960 - 120/30 = 956 and the gapped quantum value would = 4. The proposed technique also counts the number of total time-quantum consumed for the data acquisition and data missed. The value of time-quantum is defined by the doctor according to their judgment of the patients. The medical expertise would be the sole controller of the duration and starting-ending time of this time-quantum based monitoring technique for the patients individually.

A. Matrix of the COVID patients in a ward in a hospital

The serial structure of the proposed time-quantum based monitoring technique for COVID patients is indicated in Table – 1:

TABLE I

(Example of a unit of the time-quantum for continuous monitoring)

TQ	τ	τ	τ	τ	τ	τ	τ	τ	τ	τ	τ	τ	τ	τ	τ
P_2	m_{22}			m_{23}				m_{23}				m_{2u_2}			$m_{2\tau}$
P_3	m_{32}				m_{3i}			m_{33}					$m_{2\tau_3}$	m_{2u_3}	
P_4	m_{4i}			m_{42}					m_{4i}		m_{42}			$m_{2\tau_2}$	
…	…					…			…			…	…		
P_n	m_{12}		m_{1i}			m_{13}				m_{1i}			m_{1u_n}		$m_{1\tau}$

Where,

- τ = fixed range of the time-quantum for COVID patients to obtain the data as per the interval
- Y_i = i^{th} patient in the ward.
- m_{un_u} = the duration of data obtaining for the u^{th} COVID patient at its n_u^{th} interval, e.g. u^{th} patient in the $ward_1$ uses m_{un_u} unit of time-quantum (τ) at n_u^{th} duration.
- The total number of time-quantum consumed by the u^{th} patient in $ward_1$ at n_u^{th} duration is, $\frac{\sum m_{1u_n}}{\tau}$
- b_{ug_u} = the duration for not obtaining of data from the u^{th} patient at g_u^{th} duration, e.g. u^{th} patient in the $ward_1$ missed b_{ug_u} unit of time-quantum at its g_u^{th} duration.
- The total number of time-quantum missed by the u^{th} patient in $ward_1$ at g_u^{th} duration is, $\frac{\sum b_{1u_n}}{\tau}$

So, the total data collection according to the time-quantum framework for the u^{th} patient is

https://doi.org/10.36375/prepare_u.iei.a147

during this complete monitoring period, $T_u = m_{u1} + \ldots + m_{un_u} + b_{u1} + \ldots + b_{ug_u} = \sum_{i=1}^{n_u} m_{ui} + \sum_{j=1}^{g_u} b_{uj} = M_u + B_u$, where, $M_u = m_{u1} + \ldots + m_{un_u} = \sum_{i=1}^{n_u} m_{ui}$, the total unit of time-quantum consumed by the 4th patient in that duration. Now, $B_u = b_{u1} + \ldots + b_{ug_u} = \sum_{j=1}^{g_u} b_{uj}$, the total unit of time-quantum missed by the u^{th} COVID patient in that period. Now, if the missed time-quantum value, B_u for the u^{th} patient is larger than the threshold limit of adjustable tolerance for the medical practices, a notice will be issued to that doctor regarding the u^{th} patient. e.g., if data from u^{th} patient is missed for more than 5 unit of time-quantum where the threshold limit for missed time-quantum value is 4, then a warning would be generated automatically to the patients about the condition of the patients. So, the medical condition index of u^{th} patient would be calculated as, $P_u = \frac{M_u}{T_u} * 100\%$, where, T_u = total number of time-quantum assigned for the u^{th} patient. So, the number of time-quantum consumed by total COVID patients of that $ward_1$ is, $M = M_1 + M_2 + \ldots + M_u = \sum_{k=1}^{u} M_k = \sum_{k=1}^{u} \sum_{i=1}^{n_i} m_{in_i}$. And, the missed time-quantum values by all COVID patients on the same $ward_1$ is, $B = B_1 + B_2 + \ldots + B_u = \sum_{k=1}^{u} B_k = \sum_{k=1}^{u} \sum_{i=1}^{n_i} b_{in_i}$. Then, the total number of time-quantum value assigned for all the COVID patients in that $ward_1$ is, $T = M + B = (M_1 + M_2 + \ldots + M_u) + (B_1 + B_2 + \ldots + B_u) = \sum_{k=1}^{u} M_k + \sum_{k=1}^{u} B_k = \sum_{k=1}^{u} \sum_{i=1}^{n_i} m_{in_i} + \sum_{k=1}^{u} \sum_{i=1}^{n_i} b_{in_i}$.

Now, if the missed time-quantum value, B in the $ward_1$is larger than the threshold limit of tolerance, a notice will be issued to the Head of that ward automatically. Like, if $ward_1$ missed 50 units of time-quantum in total where the threshold limit is 40, then a warning will be generated automatically. So, the medical condition index of that $ward_1$ is, $\dot{b}\cdot = \cdot b / q^{\prime}$ *100%. Now, the complete time-quantum value consumed by the total wards in a hospital is, $\cdot b^{*} = \cdot b^{1} + \cdot b^{2} + \ldots + \cdot b^{h} = \sum_{i=1}^{h} \cdot b^{\hat{i}}$, and where, $\cdot b^{h}$ = the number of time-quantum consumed by that hospital. And, the total missed time-quantum by all wards in the hospital is, $\dot{b}^{*} = \dot{b}^{1} + \dot{b}^{2} + \ldots + \dot{b}^{h} = \sum_{i=1}^{h} \dot{b}^{\hat{i}}$, where, $\dot{b}^{h}$ = the number of missed time-quantum by the hospital. Then, the entire number of the time-quantum value assigned for the whole hospital is, T*=M*+B*. So, the medical condition index of that hospital is, $\dot{b}\cdot^{*} = \frac{\cdot b^{*}}{q^{\prime}}$ *100%. The graphical formation of the time-quantum value for the patients and medical data in the hospital is drawn with the variation of the 3-dimensional structure as indicated in Fig. 1:

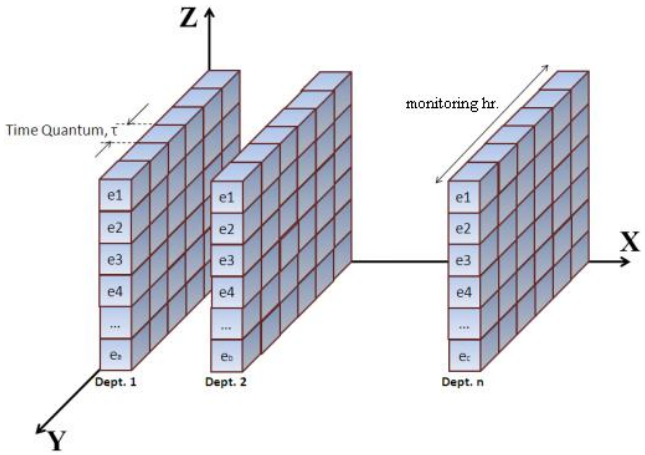

Fig. 1. Graphical representation of time quantum value with each departmental interface and employee

Where, “e1 = COVID patient 1” and “dept 1 = ward 1”, The X-axis represents the number of wards of the hospital, Y-axis represents the “monitoring time-quantum unit” defined by the hospital, Z-axis represents the number of COVID patients in the hospital, Each small box represents a single time-quantum unit (τ) assigned to the patients.

B. Data Cube representation of COVID patient’s medical condition

The basic elements in this data Tesseract represent the following parameters for the clinical measurement for the COVID patients:

- Slice: choosing of two-dimension parameters in the data cube of patients, e.g. (time-quantum, COVID patients) or (COVID patient, ward), etc.
- Dice: indicates the used quantum unit of the data cube of the patient at a certain moment. To indicate the utilized time-quantum, the value of τ = 1 and 0 for otherwise.
- Drill Down: provide detail of the total time-quantum values for each COVID patient in every ward
- Roll-up: summarize the data for the usages of time-quantum value for each patient in each ward

The graphical representation of the defined parameters mentioned above is indicated in Fig. 2:

https://doi.org/10.36375/prepare_u.iei.a147

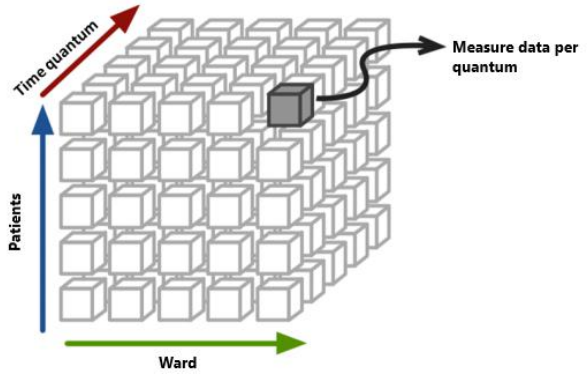

Fig. 2. Graphical representation of time-quantum unit with other dimensional factors

Where X-axis represents the number of wards of the hospital, Y-axis represents the "time-quantum unit" assigned to the patients; Z-axis represents the number of patients in the ward. The single unit of the Tesseract dice in Fig. 2 is containing the value of the clinical parameter of u^{th} patient at a particular time = m_{un_u}. So, the obtaining function for u^{th} patient in a medical ward for a certain interval of time-quantum is defined as, $fX,Y,Z = P_u$ or, where, f is also known as "Measured Value Function of the Dice" designed concerning the 3-dimensional axis of the cube model. Now, measuring the medical condition of the patients over a week, the structure of the data cube would be like as shown in Fig. 3:

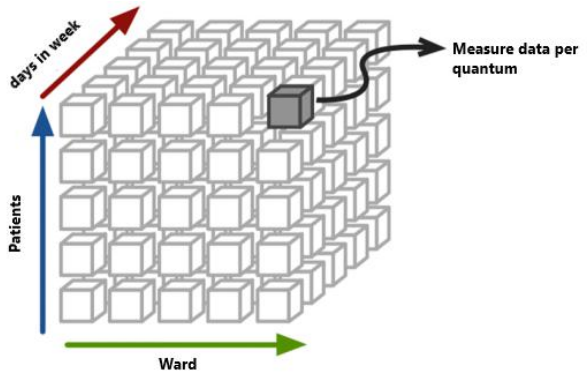

Fig. 3. Graphical representation of days in a week with various wards and patient

Where,

- The X-axis represents the number of wards of the hospital.
- Y-axis represents the monitoring days of the patients.
- Z-axis represents the number of COVID patients in the ward.

The single unit of the Tesseract dice in Fig. 3, is containing the value of the medical condition index of the u^{th} patient at that particular day = Q_u. So, the obtaining function for u^{th} patient in a particular ward for a certain day in a week is defined as, $dX,Y,Z = Q_u$ or, where, d is also known as "Measured Collective Function of the Dice" designed concerning the 3-dimensional axis of the cube model.

For the multi-dimensional data cube, Data-Tesseract is designed with the inclusion of another parameter as various departments or wards in the hospital as an additional dimension in it. For example, an additional parameter for measuring the statistical condition of the COVID hospital is the number of wards in it denoted as axis W in the structure of the following Data Tesseract along another axis {X, Y, Z} in the cube. So, in the Tesseract model along with the series of time-quantum value of the multiple patients, the various wards in hospitals and days of continuous monitoring could also be included in a single structure of the data model. The respective diagram of the Tesseract model containing all those multiple parameters: patients, time-quantum, wards, and days, is indicated in Fig. 4:

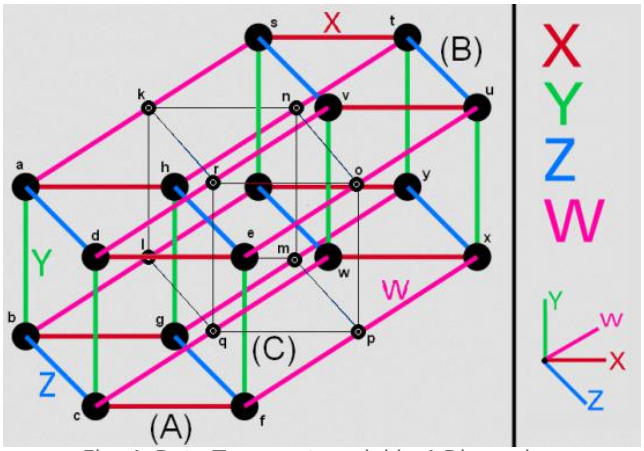

Fig. 4. Data Tesseract model in 4-Dimension

The designed structure of Data Tesseract, shown in Fig. 4, the set of three different data-cubes {A,B,C} whose coordinates are defined as, A=(a, b, c, d, e,f, g, h); B=(k, l, m, n, o, p, q, r); C=(s, t, u, v, w, x, y, z) in 3 dimensions as:

- The X-Axis represents the series of time-quantum value of such patients.
- Y-Axis represents the number of patients in a medical ward.
- Z-Axis represents the monitoring days of the patients.
- W – Axis represents the different wards of the hospital.

https://doi.org/10.36375/prepare_u.iei.a147

The above parameters could be also parameterized with another variable like different hospitals etc. taking as another dimension, Ψ – axis. The inclusion of several parameters in the data model is directly depending on the number of dimensionality of the Tesseract. For the higher dimensional data operation, the Tesseract model could be raised with another dimensionality like Ω – axis for different cities. So, it could be written as Data Tesseract = data cube ∪ extra dimensions.

Then, the detection functions for obtaining the medical condition of the u^{th} patient in a certain ward for a particular day in an identified hospital concerning the dimensionality of Tesseract model is defined as, $kX,Y,Z,W = T_u$ where k is also known as "Total Value Function of the Dice" designed concerning the multi-dimensional Tesseract model. The representation of this Tesseract for the clinical condition of the patients in vector space architecture is shown in Fig. 5:

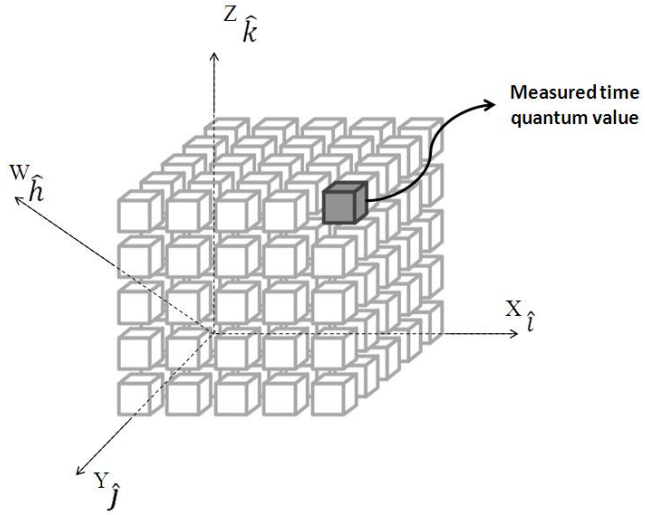

Fig. 5. Measuring of an individual time-quantum unit in 4-Dimensional data Tesseract in vector form

The multi-dimensional data Tesseract model for the monitoring of patients is calculated on the time-quantum value and medical condition index (M*, B*) stored in the unit block of data Tesseract model. Due to multiple variations in several patients, wards, days, and a series of time-quantum values, the medical condition index in the data-Tesseract model would be denoted as: $DT_{DB}xi + yj + zk + wh$, where DTDB = data point of the data Tesseract, i – Unit per time-quantum block, j – Unit per patient, k – Unit per monitoring days, h – Unit per wards.

So, the calculated value of the medical condition index for the COVID patient at a certain time-quantum phase with other the multiple factors will be indicated as:

$$P = \frac{kM_{DT_{DB}xi+yj+zk+wh}}{kT_{DT_{DB}xi+yj+zk+wh}} * 100\% = P = \frac{kM_{DT_{DB}xi+yj+zk+wh}}{kM_{DT_{DB}xi+yj+zk+wh} + B_{DT_{DB}xi+yj+zk+wh}} * 100\%$$

Where,

- P = medical condition value of the COVID patient
- $M_{DT_{DB}xi+yj+zk+wh}$ = used time-quantum slot of that COVID patient at a certain moment
- $B_{DT_{DB}xi+yj+zk+wh}$ = gapped time-quantum slot of that COVID patient at a certain moment
- k… = Total Value Function of the Dice for the patients

So, the value of the medical condition index for the b^{th} patient (y=b) on c^{th} day (z=c) of monitoring in d^{th} ward (w=d) during the a^{th} time-quantum (x=a) stamp would be stored at a certain position in the Tesseract unit indicated as $storT^* = storDT_{DB}xi + yj + zk + wh$. And, the retrieve function for that certain value from the Tesseract is denoted as $retvT^* = retvDT_{DB}xi + yj + zk + wh$. So, the foundational structure of the vector for the data Tesseract architecture is mapped between the time-quantum database to the medical condition index indicated as: $V_C l : D_c T \rightarrow P_m T$, where $V_c l$ = vector calculus, $D_c T$ = data Tesseract database, $P_m T$ = time-quantum based medical condition index. So, the representation of the Total Value Function of the Dice for the patients retrieved from the data Tesseract model is shown in Fig. 6:

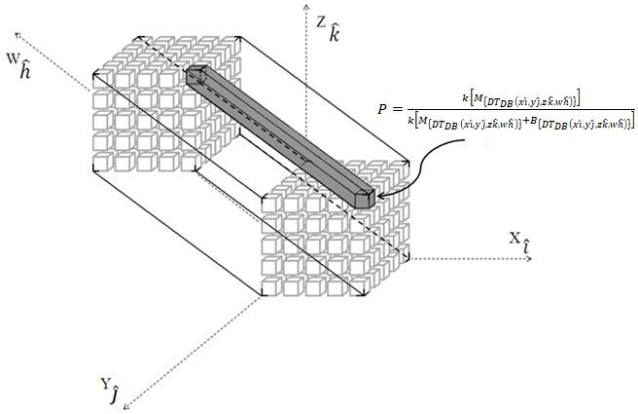

https://doi.org/10.36375/prepare_u.iei.a147

Fig. 6. Transition of a time-quantum unit in 4-Dimensional data Tesseract model

Now, the calculation of the medical condition index for a COVID patient for a complete time-quantum scale of monitoring is indicated as: $P_X = kDT_{DB}\vec{x}.i + bj + ck + dh = kM^*_X, B^*_X$, where:

- P_X = medical condition of a COVID patient for a complete time-quantum scale of monitoring
- M^*_X = total number of time-quantum used by that COVID patient for a complete time-quantum scale of monitoring
- B^*_X = total number of time-quantum missed by that COVID patient for a complete time-quantum scale of monitoring

Designing of the Proposed Technique

The implementation of the proposed multi-dimensional Tesseract model is initially applied to the twin medical dataset of COVID patients obtained from Kaggle. One dataset contains the physiological temperature value of the COVID patients and the other does not. There are two CSV (Comma Separated Value) files that have been acquired in this study and executed in Python. The code for visualization of data is written and implemented in Python 3.8.2 in a Core 2 duo processor-based system on a 64-bit Windows 10 platform with the help of 4 Gb RAM.

In both CSV files, all the physiological parameters used in the medical study of the COVID patients are almost identical. Those CSV files are then analytically visualized in the online RAWGraph portal and diagnostic XLStat tool in a windows office suit. The multi-dimensional plotting visualization of the medical data of the COVID patients for dataset – 1 and 2 executed in Python is shown in Fig. 7:

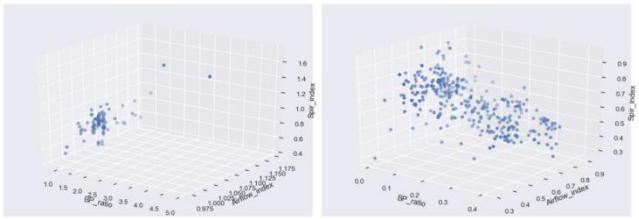

Fig. 7. Discrete variation of plotting of medical data of COVID patients

In Fig. 7, both images indicate the discrete variation of plotting of medical data of COVID patients where the axis is denoted as BP_ratio (X-axis), Airflow index (Y-axis), and Spir_index (Z-axis). The multi-dimensional contour visualization of the medical data of the COVID patients for dataset – 1 and 2 executed in Python is shown in Fig. 8:

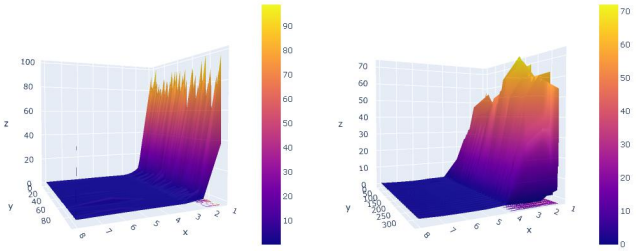

Fig. 8. Continuous contour variation of medical data of the COVID patients

In Fig. 8, both images indicate the continuous contour variation of medical data of the COVID patients where the axis is denoted as: no. of medical parameters (X-axis), no. of COVID patients (Y-axis) and values of those parameters (Z-axis). The 3-dimensional visualization of the medical data of the COVID patients for dataset – 1 and 2 executed in XLStat is shown in Fig. 9:

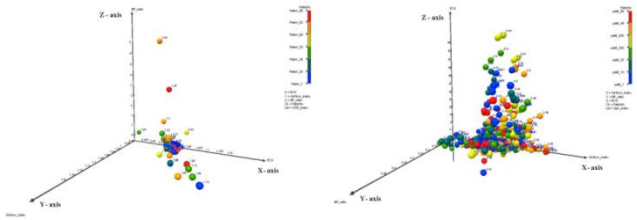

Fig. 9. Different scatter plot distribution of COVID patients for dataset – 1 and 2 concerning temperature

In the left part of Fig. 9, the color variation indicates the orientation of the temperature value of patients concerning different axis: ECG (X-axis), Airflow index (Y-axis), and BP ratio (Z-axis). The numerical indication at each plot mentions the GRS factor of each patient. And in the right part of Fig. 9, the color variation indicates the orientation of the patients concerning different axis: Airflow index (X-axis), BP ratio (Y-axis), and ECG (Z-axis). And the numerical indication at each plot mentions the SPiR factor of each patient. The simulation of the medical data of the COVID patients for the dataset-1 performed in XLStat is executed by the proposed three-dimensional graphical modelling as indicated in Fig. 10:

https://doi.org/10.36375/prepare_u.iei.a147

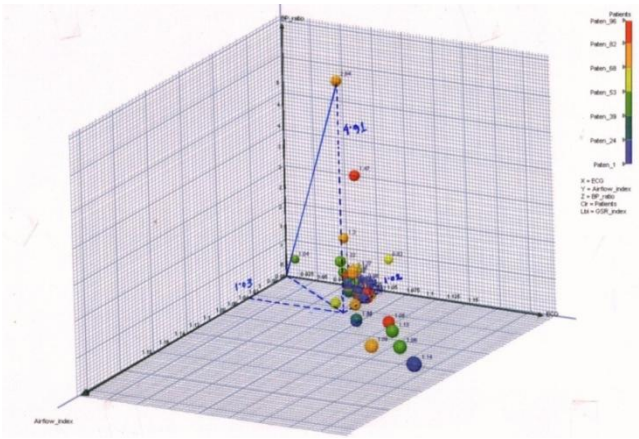

Fig. 10. 3-D graphical representation of the COVID patients of the dataset – 1

In Fig. 10, the 3-dimensional graphical representation of the COVID patients of the dataset – 1 is designed for the GSR_index value = 2.64, the respective values are: ECG = 1.02, Airflow_index = 1.03, BP_ratio = 4.91 and patient category between no. 68 to 82. The simulation of the medical data of the COVID patients for the dataset-1 performed in XLStat is executed by the proposed three-dimensional graphical modelling as indicated in Fig. 11:

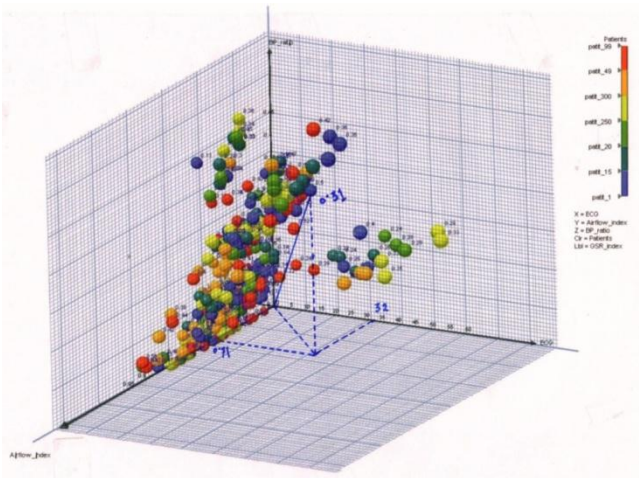

Fig. 11. 3-D graphical representation of the COVID patients of the dataset – 2

In Fig. 11, the 3-dimensional graphical representation of the COVID patients of the dataset-2 is for the GSR_index value = 0.5, the respective values are: ECG = 32, Airflow_index = 0.71, BP_ratio = 0.31 and patient category between no. 0 to 15. With this technique the resulted plots of the graphs generated from the XLStat is linked with an additional dimension with each other. The simulation of the connective aspect between the dataset-1 and 2 of the COVID patients performed in XLStat is executed by the proposed multi-dimensional graphical modelling technique as indicated in Fig. 12:

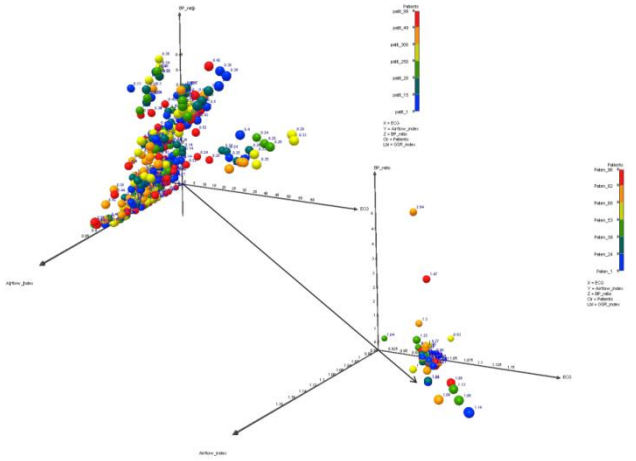

Fig. 12. 4-D Tesseract model-based representation of medical dataset – 1 and 2

In Fig. 12, the complete image indicates 4-dimensional Tesseract model-based representation of medical data of the COVID patients where the axis are denoted as the dimensionality is represented according to the BP_ratio and ECG of the COVID patients, a variation of colours represents temperature differences of COVID patients and the extra-dimensional line denotes the variation of wards in the hospital. The multi-dimensional visualization of the medical data of the COVID patients of the dataset-1 executed in XLStat is shown in Fig. 13 after subdivided into two uniform sub-wards:

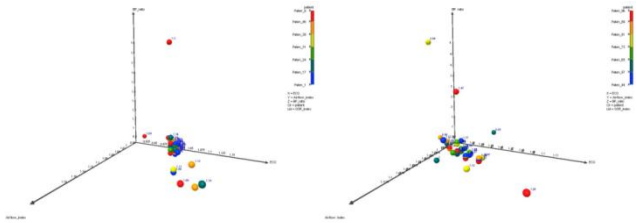

Fig. 13. Distribution of temperature value of patients in a dataset – 1 into two uniform subdivisions

In the left part of Fig. 13, the colour variation indicates the orientation of the temperature value of patients concerning different axis: ECG (X-axis), Airflow index (Y-axis), and BP ratio (Z-axis). The numerical indication at each plot mentions the GRS factor of each patient. And in the right part of Fig. 13, the colour variation indicates the orientation of the patients concerning different axis: Airflow

https://doi.org/10.36375/prepare_u.iei.a147

index (X-axis), BP ratio (Y-axis), and ECG (Z-axis). And the numerical indication at each plot mentions the SPiR factor of each patient. In Fig. 26, the sub-divisional factor is oriented with all the parameters of the COVID medical data and its respective patients uniformly. The simulation of the 1st part of the subdivided medical dataset – 1 for the forty-six COVID patients performed in XLStat is executed by the proposed three-dimensional graphical modelling as indicated in Fig. 14:

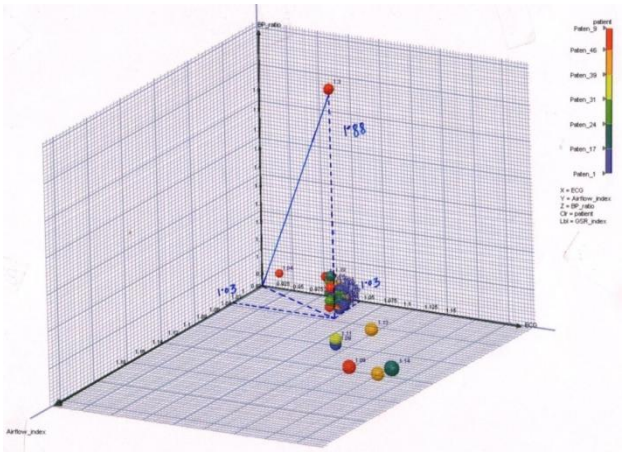

Fig. 14. 3-D graphical representation of the COVID patients for 1st part of dataset – 1

In Fig. 14, the 3-dimensional graphical representation of the COVID patients subdivided into two uniform smaller wards from patient - 1 to patient - 46 in dataset – 1 is designed for the GSR_index value = 1.3, the respective values are: ECG = 1.03, Airflow_index = 1.03, BP_ratio = 1.88 and between the patient category from no. 39 to 46. The simulation of the 2nd part of the subdivided medical dataset – 1 for another forty-six COVID patients performed in XLStat is executed by the proposed three-dimensional graphical modelling as indicated in Fig. 15:

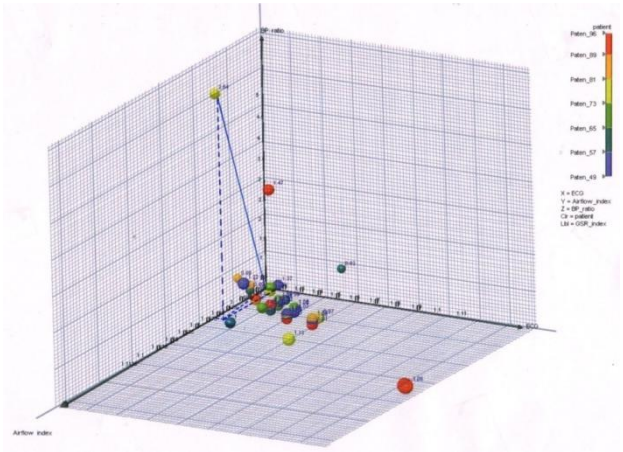

Fig. 15. 3-D graphical representation of the COVID patients for 2nd for dataset – 2

In Fig. 15, the 3-dimensional graphical representation of the COVID patients subdivided into two uniform smaller wards from patient - 1 to patient - 46 in dataset – 1 is designed for the GSR_index value = 2.64, the respective values are: ECG = 1.02, Airflow_index = 1.03, BP_ratio = 4.91 and between the patient category from no. 73 to 81. With this technique the resulted plots of the graphs generated from the XLStat is linked with an additional dimension with each other. The simulation of the connective aspect between the subdivided datasets of dataset-1 of the COVID patients performed in XLStat is executed by the proposed multi-dimensional graphical modelling technique as indicated in Fig. 16:

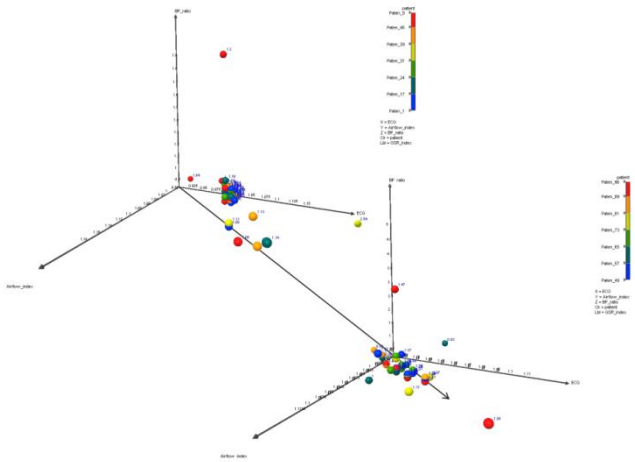

Fig. 16. 4-D Tesseract model-based representation of medical dataset – 1 subdivided

In Fig. 16, the complete image indicates 4-dimensional Tesseract model-based representation of medical data of the COVID

https://doi.org/10.36375/prepare_u.iei.a147

patients where the axis are denoted as the dimensionality is represented according to the BP_ratio and ECG of the COVID patients, a variation of colors represents temperature differences of COVID patients and the extra-dimensional line denotes the variation of wards in the hospital where the dataset – 1 is divided into two uniform sub-wards. The directive relation between medical dataset – 1 with its subdivisions simulated by the proposed 4-dimensional Tesseract based graphical structures and performed in XLStat is shown in Fig. 17:

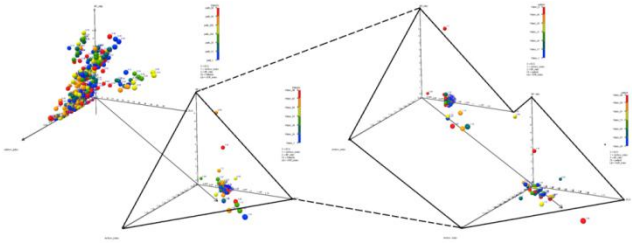

Fig. 17. Relation between the 4-D Tesseract models and sub-division of dataset – 1

In Fig. 17, the complete image indicates the relation between the 4-dimensional Tesseract models based representation of medical data of the COVID patients for dataset – 1, 2 and the sub-division of wards for the dataset – 1 into two uniform sub-wards in the hospital.

A. Effectiveness of the proposed modelling

The efficiency of the proposed model is evaluated on the 3-dimentional graphical structure model instead of numerical valuation method. So, the measurement of the competence is modelled through the simulated relation between the dataset: 1 – 2 and subdivided datasets. The connective 3-dimentional representation of the medical dataset-1 and 2 according to the simulated 4-dimensional Tesseract based graphical model and performed in XLStat is shown in Fig. 18:

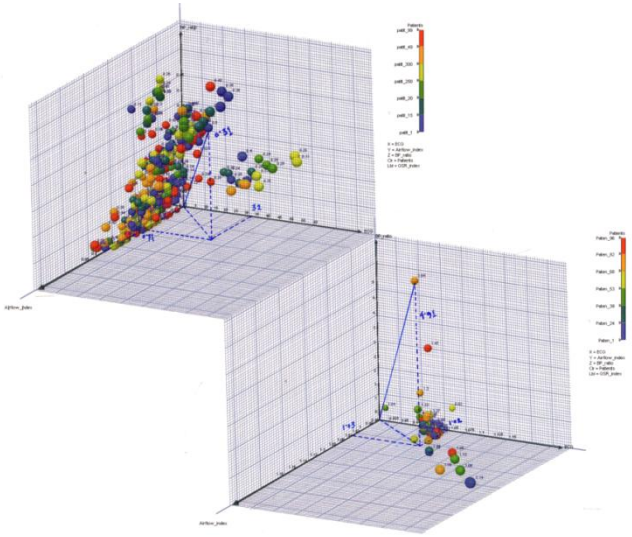

Fig. 18. Combined 4-D representation of the COVID patients for both dataset-1 and 2

In Fig. 18, the combined image indicates 4-dimensional graphical representation of the COVID patients for both dataset-1 and 2 with respect to the Tesseract model where the extra-dimension graphical structure denotes the variation of wards in the hospital. The connective 3-dimentional representation of the subdivision of the medical dataset-1 according to the simulated 4-dimensional Tesseract based graphical model and performed in XLStat is shown in Fig. 19:

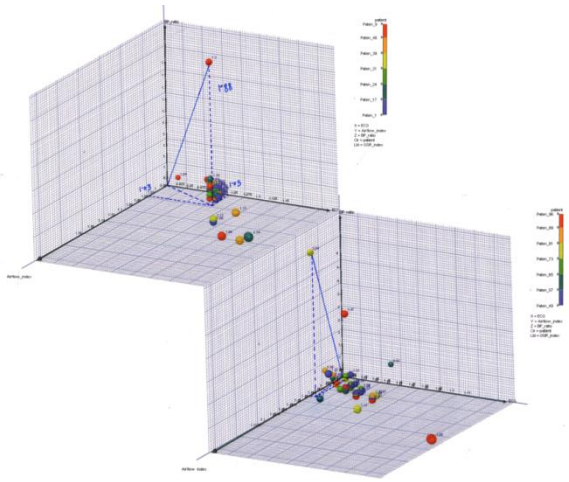

Fig. 19. 4-D Tesseract model based graphical representation of dataset – 1 subdivided

In Fig. 19, the combined image indicates 4-dimensional graphical representation of the COVID patients for the dataset-1 with respect to the Tesseract model where the extra-dimension graphical structure denotes the division of two uniform sub-wards in the

hospital. The directive combination between medical dataset – 1 with its subdivisions simulated by the proposed 4-dimensional Tesseract based graphical technique and performed in XLStat is shown in Fig. 20:

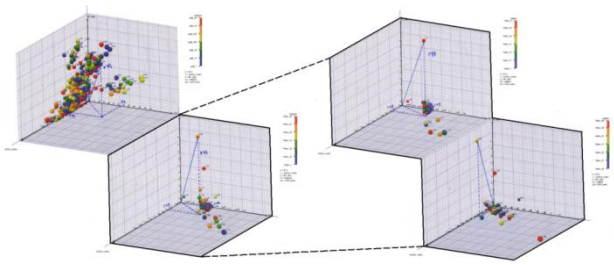

Fig. 20. Relation between the 4-D Tesseract graphical models & subdivision of dataset – 1

In Fig. 20, the complete image indicates the relation between the 4-dimensional Tesseract models based 3-D graphical representation of medical data of the COVID patients for dataset – 1, 2 and the sub-division of wards for the dataset – 1 into two uniform sub-wards in the hospital.

B. Numerical comparativeness

The numerical comparative efficiency of the COVID dataset – 1 and 2 with the subdivision of the datasets 1 are calculated with respect to the numerical values measured in the simulated 3-dimentional graphs. The average value and the error difference of the clinical parameters of the subdivided datasets with respect to the dataset 1 are indicated in Table 2:

TABLE I
(NUMERICAL CALCULATION OF THE MEASURED CLINICAL PARAMETERS)

Type	ECG	Airflow	BP ratio	GSR index
Measured value	1.02	1.03	4.91	2.64
Calculated value	1.025	1.03	3.395	1.97
Error Difference	0.005 ≃ 0	0.0	1.51	0.67
Percentage of error	0	0	44.47	34.01

The error values of the COVID patients' clinical parameters measured by the proposed model is varies in division. The error calculation of the ECG and the airflow parameters of the patients is zero. But the error value of the BP ratio and GSR index is 44.47% and 34.01% respectively. So, the average value of the percentage of error is $\frac{55/58,\ 45/12,\ 1,\ 1}{5}$ = 19.62%. From this observation, it could be concluded that multidimensional visualization is mainly works on non-dependable clinical parameters. Due to more fluctuation on BP ratio and GSR index for health measurements, the error is instable and oscillates with respect to more clinical parameters of the COVID disease.

CONCLUSION

This technique is strictly based on time-divisional approach which mainly considered the multivariate statistical parameters of clinical inferences. The medical conditions of COVID patients' measured by different sensors and devices are exercised through multidimensional data architecture model for both doctors and hospital perspectives. This analysis of the COVID patients' dataset had been structured with the help of visualization technique in XLStat tool. The interconnectivity between the doctors and hospital authorities would be minimized for fundamental accesses. By this technique, one's data could not only be subdivided into multiple parts or integrated multiple factors into one block but also the overall scenario of COVID could also be examined by expertise easily. In other words, the management and doctors both could visualize and manage the data according to their requirements. The monitoring of the patients by this system could also allow the facility manager to prevent any further contaminative situation in the hospital. So, it would be obvious that an intelligent and robust visualization method would be required for further visual scrutiny to understand the status of the COVID scenario better definitely for both the stakeholders.

ACKNOWLEDGMENT

This experiment is conducted under the Fellowship of the Post-Doctoral Research in the National Institute of Technology, Trichy, TN – 620015, India.

REFERENCES

[1] Biruk, Senafekesh, Tesfahun Yilma, Mulusew Andualem, and Binyam Tilahun. "*Health Professionals' readiness to implement electronic medical record system at three hospitals in Ethiopia: a cross sectional study.*" BMC medical informatics and decision making 14, no. 1 (2014): 115.

[2] Sporici, Dan, Elena Cușnir, and Costin-Anton Boiangiu. "*Improving the Accuracy of Tesseract 4.0 OCR Engine Using Convolution-Based Preprocessing.*" Symmetry 12, no. 5 (2020): 715

[3] Kim, Y. K., H. Wang, and M. S. Mahmud. "*Wearable body sensor network for health care applications.*" In

Smart Textiles and their Applications, pp. 161-184. Woodhead Publishing, 2016.
[4] Cao, Yunshan, Nan Wang, Hong Peng, Quanying Liu, and Wenyu Cao. "*Information technology and health care: A scenario of biofeedback.*" In 5th International Conference on Pervasive Computing and Applications, pp. 50-55. IEEE, 2010.
[5] Dash, Sabyasachi, Sushil Kumar Shakyawar, Mohit Sharma, and Sandeep Kaushik. "*Big data in healthcare: management, analysis and future prospects.*" Journal of Big Data 6, no. 1 (2019): 54.
[6] Romano, Rosalba, and Emilia Gambale. "*Statistics and medicine: the indispensable know-how of the researcher.*" Translational Medicine@ UniSa 5 (2013): 28.
[7] Jones, B. E., and M. A. Ould. "*The patient medical record as a database.*" The Computer Journal 17, no. 4 (1974): 295-301.
[8] Vuma, Sehlule, and Bidyadhar Sa. "*A comparison of clinical-scenario (case cluster) versus stand-alone multiple choice questions in a problem-based learning environment in undergraduate medicine.*" Journal of Taibah University Medical Sciences 12, no. 1 (2017): 14-26.
[9] Gong, Jingjing, Yan Zhang, Zheng Yang, Yonghua Huang, Jun Feng, and Weiwei Zhang. "*The framing effect in medical decision-making: a review of the literature.*" Psychology, health & medicine 18, no. 6 (2013): 645-653.
[10] Simon, H., H. Guetzkow, K. Kozmetsky, G. Tyndall, (1954) "*Centralization vs. decentralization in organizing the controller's department*", paper, Controllership Foundation,
[11] Francis, J. L., and T. R. P. Martin. "*8 Principles of interfacing computers to medical equipment.*" Baillière's clinical obstetrics and gynaecology 4, no. 4 (1990): 787-795.
[12] Plageras, Andreas P., Christos Stergiou, George Kokkonis, Kostas E. Psannis, Yutaka Ishibashi, Byung-Gyu Kim, and B. Brij Gupta. "*Efficient large-scale medical data (ehealth big data) analytics in internet of things.*" In 2017 IEEE 19th Conference on Business informatics (CBI), vol. 2, pp. 21-27. IEEE, 2017.
[13] Simons R., (2000) "*Performance measurement and control systems for implementing strategy: text & cases*", Prentice-Hall, Upper Saddle River, NJ, USA.
[14] Sidek, Yusof Haji, and Jorge Tiago Martins. "*Perceived critical success factors of electronic health record system implementation in a dental clinic context: an organisational management perspective.*" International Journal of Medical Informatics 107 (2017): 88-100
[15] Zozus, Meredith N., Carl Pieper, Constance M. Johnson, Todd R. Johnson, Amy Franklin, Jack Smith, and Jiajie Zhang. "*Factors affecting accuracy of data abstracted from medical records.*" PloS one 10, no. 10 (2015): e0138649.
[16] Quantum Client Briefing, (1973) "*Customised Organisational Action Research*", Quantum Management, Indicators.
[17] Cook, Robert J., and Steven J. Durning. "*Clinical Process Modeling: An Approach for Enhancing the Assessment of Physicians' Clinical Reasoning.*" Academic Medicine 94, no. 9 (2019): 1317-1322.
[18] Black, David R., Daniel C. Coster, and Samantha R. Paige. "*Physiological health parameters among college students to promote chronic disease prevention and health promotion.*" Preventive medicine reports 7 (2017): 64-73.
[19] Kakria, Priyanka, N. K. Tripathi, and Peerapong Kitipawang. "*A real-time health monitoring system for remote cardiac patients using smartphone and wearable sensors.*" International journal of telemedicine and applications 2015 (2015).
[20] Client Case Studies - Vol. 1, (2009) Profiles Research Institute, Waco, Texas, USA.
[21] Malykh, V. L., and S. V. Rudetskiy. "*Approaches to medical decision-making based on big clinical data.*" Journal of healthcare engineering 2018 (2018).
[22] Cleary, Timothy J., Abigail Konopasky, Jeffrey S. La Rochelle, Brian E. Neubauer, Steven J. Durning, and Anthony R. Artino. "*First-year medical students' calibration bias and accuracy across clinical reasoning activities.*" Advances in Health Sciences Education 24, no. 4 (2019): 767-781
[23] Tang, Jing, Hengqing Tong, Hui Peng, and Yang Liu. "*Ubiquitous Intelligent Monitoring System in Psychological Health.*" In 2008 2nd International Conference on Bioinformatics and Biomedical Engineering, pp. 1371-1374. IEEE, 2008.
[24] Simmons, H. E., and R. E. Merrifield. "*Mathematical description of molecular structure: Molecular topology.*" Proceedings of the National Academy of Sciences 74, no. 7 (1977): 2616-2